

Electric-field-control of electromagnons' frequency in multiferroics

S. Omid Sayedaghaee,¹ Charles Paillard,² Sergey Prosandeev,¹

Sergei Prokhorenko,¹ Yousra Nahas,¹ Bin Xu,³ and L. Bellaiche¹

¹*Physics Department and Institute for Nanoscience and Engineering,
University of Arkansas, Fayetteville, Arkansas 72701, USA*

²*Laboratoire Structures, Propriétés et Modélisation des Solides,
CentraleSupélec, CNRS UMR 8580,*

Université Paris-Saclay, 91190 Gif-sur-Yvette, France

³*Institute of Theoretical and Applied Physics
and School of Physical Science and Technology,
Soochow University, Suzhou, Jiangsu 215006, China*

(Dated: October 25, 2022)

Abstract

Electromagnons, which are coupled polar and magnetic excitations in magnetoelectric materials, are of large interest for electronic and computing technological devices. Using Molecular Dynamics simulations based on an *ab-initio* effective Hamiltonian, we predict that the frequency of several electromagnons can be tuned by the application of electric fields in the model multiferroic BiFeO₃, with this frequency either increasing or decreasing depending on the selected electromagnon. In particular, we show that the frequency of electromagnons localized at ferroelectric domain walls can be tuned over a 200 GHz range by realistic dc electric fields. We interpret the realized frequency increase (respectively, decrease) by local hardening (respectively, softening) of the associated polar phonons which couples to the applied electric field. The increase *versus* decrease of the electromagnons' frequency is further found to be correlated with the real-space localization of such phonons.

I. INTRODUCTION

Electromagnons, a coupled oscillation wave of electrical and magnetic dipoles in magnetoelectric materials, have bolstered large interest since they were first discussed in 1970s [1, 2]. They have remained elusive for a long time, except in a few materials such as rare-earth (R) manganites RMnO₃ [3–5], RMn₂O₅ [6, 7] or ferrite perovskite oxides [8–11]. Among them, BiFeO₃, a room temperature multiferroic [12], has been one of the most intensely considered magnetoelectrics for electromagnon detection, characterization and technological applications. Among the various experimental and theoretical studies of electromagnons, most have focused on so-called electro-active magnons, *i.e.*, control of spin waves by electric fields [13–17]. On the other hand, much less work has been devoted to the study of magnetic control of polarization waves, with a few theoretical works realized in BiFeO₃ [18–20] and manganites [21]. The present work goes one step further by bridging the two approaches, as we intend to demonstrate the possibility of resonantly exciting electromagnons (induced by ferroelectric domain walls) using ac magnetic fields while concurrently manipulating their frequency with dc electric fields.

Note that ferroelectric domain walls can now routinely be written, erased and reconfigured using, for instance, PiezoForce Microscopy [22–25]. The ability to generate magnetically polarization waves localized at domain walls, as proposed in Ref. [18], already promises the

tantalizing possibility of reconfigurable nanometer size electrical circuits, whose power is switched on and sustained remotely by ac magnetic fields. If now one is able to act on the electrical polarized waves localized at the ferroelectric domain walls, for instance using local electric fields, one could dream of achieving reconfigurable logical elements for computing or detection.

In this work, we investigate how dc electric fields affect the domain-wall-induced electromagnons evidenced in Ref. [18] in multiferroic BiFeO₃. Using Molecular Dynamics based on an *ab-initio* effective Hamiltonian, we reveal that the frequency of these electromagnons is rather sensitive to these dc fields, either increasing or decreasing with them depending on the chosen electromagnon. This latter different behavior (namely, increase *versus* decrease) is found to be correlated with the real-space localization of the optical phonon associated with these electromagnons.

II. METHODS

Here and as shown in Figure 1, we simulate a multidomain system of BFO with 180° domain configuration inside which two types of domains alternate along the [110] pseudo-cubic direction. The first type of domain, denoted as *D1*, is shown in red in Fig. 1 and possesses electric dipoles aligned along the $[\bar{1}11]$ direction. The second kind of domain, coined *D2*, is displayed in blue in this figure and exhibits electric dipoles lying along the opposite $[1\bar{1}\bar{1}]$ direction. In both domains the magnetic moments and antiferromagnetic (AFM) moments are along the perpendicular $[211]$ and $[0\bar{1}1]$ directions, respectively.

The energetics and properties of the studied system are modeled via the use the effective Hamiltonian framework detailed in Ref. [26] within a molecular dynamics (MD) approach [27], in order to obtain dynamical properties. Technically, Newtonian equations of motion are used to investigate the dynamics of the ionic degrees of freedom of this effective Hamiltonian – that are local modes which are directly proportional to local electric dipoles inside each 5-atom cell; pseudo-vectors representing the antiferrodistortive motions inside such 5-atom cells; and both homogeneous and inhomogeneous strain components. Regarding the dynamics of the magnetic moments, the approach of Ref. [28] is followed, for which such dynamics are treated through the Landau-Lifshitz-Gilbert (LLG) equation [29].

DC electric fields with magnitude ranging between 1.0×10^7 V/m and 1.0×10^8 V/m

are applied along the $[\bar{1}11]$ direction to such multidomain, that is currently mimicked by using a $24 \times 24 \times 6$ supercell. It should be noted that an electric field of the magnitude of 2.0×10^8 V/m is strong enough to reorient all dipole moments along its direction and convert the configuration to monodomain. The MD simulations are conducted at the temperature of 10 K. To ensure that the magnetic moments only slightly fluctuate about the same direction during the course of simulations, a dc magnetic field of the magnitude of 245 T is applied along the $[211]$ direction. A lower magnetic field (which is accessible in practical applications) could be applied. In fact, we also performed simulations with a *dc* magnetic field having a magnitude of 2.45 T along the $[211]$ direction, and obtained similar results. Such a large magnetic field along with low temperature were chosen here to avoid large fluctuations of magnetic properties and see the results more clearly. Each MD simulation was performed for 1,000,000 steps of 0.5 fs each, while both homogeneous and inhomogeneous strains were relaxed.

III. RESULTS AND DISCUSSION

It is important to realize that, under zero dc electric field, there is no macroscopic polarization, as a result of the cancellations between the polarizations of the $D1$ and $D2$ domains. On the other hand, we numerically found that the application of our considered dc electric fields results in the increase of the magnitude of electric dipoles in the $D1$ regions and its reduction in the $D2$ areas, therefore yielding now a finite overall polarization along the direction of the applied field which is $[\bar{1}11]$. It is worth mentioning that we observed the change in the structure from a 180-degree multidomain to a monodomain when the applied electric field exceeds a threshold ($E_{threshold} = 2 \times 10^8$ V/m) which is rather abrupt - at least with the resolution of the applied electric field change here, being $E = 1 \times 10^7$ V/m. One may thus need a much smaller step in field's magnitude to observe motion of the domain walls. One can also increase the temperature to see such motion. For instance, and as shown in the Supplementary Material, motion of the domain walls does occur at $T = 300$ K when the applied electric field varies from $E = 3 \times 10^7$ V/m to $E = 5 \times 10^7$ V/m.

We then perform Fourier analysis of the temporal evolution of this resulting electrical polarization along the $[\bar{1}11]$ direction, and that of the magnetization along the $[211]$ direction. Figure 2 shows the resulting Fast Fourier Transformations (FFT) of both the electrical

polarization and magnetization for a dc electric field of 1.0×10^7 V/m, which reveals the
 existence of frequency modes presenting phonons and magnons. Here, in particular, some
 peaks are observed at the same frequency in the FFT spectrum of both polarization and
 magnetization, which is a signature of electromagnons. Within the electromagnonic modes
 that are observed here, four modes are of particular interest due to their noticeable frequency
 shift as a response to the application of electric fields of various magnitudes. These modes
 are denoted by Mode 1, Mode 2, Mode 3, and Mode 4 in Figure 2 (Note that these four
 modes have very similar frequencies than those one can guess to be around 90 cm^{-1} (\simeq
 2700 GHz) and 140 cm^{-1} ($\simeq 4200 \text{ GHz}$) in the Supplemental materials of Ref. [30] for
 precisely 180° domains of BFO). The electric-field-induced frequency shift of both the phonon
 and magnon associated with the electromagnonic Mode 1 is demonstrated in Figs. 3a and
 3b, respectively. For this mode, as indicated by purple solid lines in Figs. 3a and 3b,
 when the applied electric field is 1.0×10^7 V/m the phonon peak is at 2490 GHz (Figure
 3a) and the magnon peak is exactly at the same frequency location (Figure 3b). When
 the applied electric field increases to higher magnitudes, the frequency of the phonon and
 magnon decrease concurrently which results in a softening for Mode 1. It should be noted
 that, in multiferroics, strain can contribute to the emergence of so-called electroacoustic
 magnons as a mixture of acoustic phonons, optical phonons, and magnons [19, 20]. Here,
 we numerically found (not shown here) that the four aforementioned modes are present in
 the frequency spectrum of both the polarization and magnetization even if the homogeneous
 strain is clamped during the course of MD simulations, which clarifies that these modes are
 electromagnons consisting of optical phonons and magnons. *It should be noted that we
 do not believe that these computed intensities of Figure 3 have a real physical meaning in
 our simulations, since such intensities are not monotonic with the fields and can vary when
 slightly changing some technical details of the Fourier Transform (especially, considering the
 small values of the vertical scale in the Figure). On the other hand, the frequency position
 of these peaks is insensitive to such details and does carry physical significance.*

For each of these four considered modes, the evolution of their frequency as a function
 of the magnitude of the dc electric field is shown in Figure 4. One can see that Mode
 1 experiences a rather strong decrease of its frequency when the electric field varies from
 1.0×10^7 V/m to 1.0×10^8 V/m, namely by about 200 GHz from 2490 GHz to 2290 GHz .
 Note that it is known that the effective Hamiltonians of BFO overestimate the magnitude

of electric fields by a factor of 23 [31]. Hence, our maximum applied electric field would correspond experimentally to approximately 43 kV/cm, which is easily sustained in BiFeO₃ thin films [32]. Note also that the decrease of the Mode 1 frequency appears to be quadratic in nature. Mode 2 also adopts a reduction of its frequency, but at a smaller extent (that is by about 55 GHz from 2715 GHz to 2660 GHz) and in a linear fashion, with a rate of 0.06 GHz/(kV/cm). Interestingly, such linear variation has indeed been observed in BiFeO₃ for some electromagnons. For instance, the frequency of the so-called extra-cyclon mode ψ_2 may increase or decrease (depending on whether the electric field increases or decreases the polarization) with a rate of approximately 1.3 GHz/(kV/cm) [33]. In the same reference, the cyclon mode ϕ_2 shows an opposite behavior with an electrical rate of control of the magnon frequency of ≈ 0.24 GHz/(kV/cm). Note that we focus here on domain-wall-induced electromagnons with an antiferromagnetic structure, while the cyclon and extra-cyclon modes considered in Ref [33] are modes in a monodomain single crystal having a magnetic cycloidal state. In addition, the commonly known overestimation of electric fields in effective Hamiltonian models may also contribute to the difference between computational and experimental rates for the dc-field-induced change in frequency. As a matter of fact, rescaling our theoretical fields by dividing them by 23 (as indicated in Ref. [31]) results in a rate for our Mode 2 that goes from 0.06 GHz/(kV/cm) to 1.38 GHz/(kV/cm), which is similar to the observed magnitude of such rate for the ψ_2 mode in Ref [33]. Similarly, Mode 3 has the same kind of qualitative behavior than Mode 2 but with about twice the slope – that is, a linear decrease of its frequency by $\simeq 117$ GHz when the *dc* electric field strengthens from 1.0×10^7 V/m to 1.0×10^8 V/m. Strikingly, Mode 4, whose frequency is basically that of Mode 3 for an interpolated zero field, adopts a mirror behavior with respect to Mode 3, in the sense that its frequency concomitantly linearly increases by a similar amount of $\simeq 117$ GHz. Note that we also performed simulations with *opposite dc* electric fields (i.e., along $[1\bar{1}\bar{1}]$), which allows us to further determine that the frequencies of Modes 1 and 2 depend on the *magnitude* of the electric field along $[\bar{1}11]$ or $[1\bar{1}\bar{1}]$ while those of Modes 3 and 4 linearly depend on the *projection* of the electric field along $[\bar{1}11]$ (i.e., on the magnitude but also sign of this projection).

In order to understand all these behaviors and demonstrate their relationship with real-space localization, a layer-by-layer analysis is performed at the different planes that are parallel to the domain wall. More precisely, the Fourier transform of the average of po-

larization of each of these planes is computed for the frequencies associated with the four
aforementioned modes for a dc field of 1.0×10^7 V/m, and is shown in Figure 5. For instance,
Panel (a) of Figure 5 tells us that Mode 1 is a mode that is strongly localized at the domain
walls. Furthermore, Panel (b) of Figure 5 reveals that Mode 2 also localizes near the domain
walls but to a smaller extent, as seen by comparing its vertical scale with that of Figure
5(a). Consequently, by looking at Figs 4(a), 4(b), 5(a) and 5(b), one can conclude that
modes localizing near the domain walls soften under a *dc* electric field, that is they have
their frequency decreasing when the field increases – and such decrease is larger when the
localization near the walls is stronger.

Interestingly, Figures 5(c) and 5(d) tell us that Modes 3 and 4 are rather different from
Modes 1 and 2, in the sense that they prefer to localize inside the domains rather than at
the domain walls. More precisely, Mode 3 reaches its maximum of the Fourier transform
of the polarization in the *D2* region inside which the polarization is antiparallel to the
applied electric field. Consequently, applying such field will decrease the magnitude of the
polarization in the *D2* area, which corresponds to a local softening of the optical phonon,
hence explaining the decrease of the frequency seen in Fig. 4c for Mode 3. In contrast,
Mode 4 preferentially localizes in the *D1* area for which the polarization is parallel to the
dc electric field, and, as a result, such polarization increases in magnitude when the field
strengthens. Such increase leads to a local hardening of Mode 4, therefore to a frequency
that now increases with the field. Note that Modes 3 and 4 (whose frequency are about
4210 GHz and 4245 GHz for a field of 1.0×10^7 V/m, which correspond to 140 cm^{-1} and
 142 cm^{-1} , respectively) can be thought as both originating from the known zone-center optical
phonon of BiFeO₃ monodomain, that then splits in two under dc electric fields because of the
existence of domain walls and two different types of domains in our studied system. Based
on previous works on BiFeO₃ monodomain single crystals and the fact that we numerically
further found (not show here) that Modes 3 and 4 have rather small FFT of the component
of the polarization along the [110]-direction (which is perpendicular to the polarizations of
both D1 and D2), one can suggest that Modes 3 and 4 originate from the $A_1(LO)$ mode,
rather than the $E(TO)$ mode, of BiFeO₃ monodomain [28, 34–37].

IV. SUMMARY

In summary, we used an atomistic effective Hamiltonian to reveal that the frequency of electromagnons can be significantly tuned by applying dc electric fields in the prototypical BiFeO_3 multiferroic adopting ferroelectric domains. Such finding is promising towards the design of novel devices taking advantage of the dual electric and magnetic natures of electromagnons, with the additional conveniences demonstrated here that (1) it should thus be possible to select the desired operating frequency by choosing the right combination of ac magnetic field's frequency and magnitude of the dc electric field (in order to activate such electromagnons at this desired frequency); and (2) some of these electromagnons are localized at the ferroelectric domain walls, therefore rendering feasible the application of local electric fields for realizing reconfigurable logical elements for computing or detection. These domain-wall-induced electromagnons are further found to either increase or decrease their frequencies under the dc electric fields, depending on the real-space localization of their associated phonons— that is at the ferroelectric domain walls or at the “up” *versus* “down” domains. We therefore hope that the present study deepens the fascinating fields of electromagnons, ferroelectric domains and magnonics.

ACKNOWLEDGEMENTS

The authors thank the Vannevar Bush Faculty Fellowship (VBFF) Grant No. N00014-20-1-2834 from the Department of Defense and the ARO Grant No. W911NF-21-1-0113. C.P. thanks the ANR Grant No. ANR-21-CE24-0032 SUPERSPIN, and a public grant overseen by the ANR as part of the Investissements d’Avenir program (Reference: ANR-10-LABX-0035, Labex-NanoSaclay). S.P. also acknowledges ONR Grant No. N00014-21-1-2086. B.X. further acknowledges the financial support from National Natural Science Foundation of China under Grant No. 12074277, the startup fund from Soochow University, and the support from Priority Academic Program Development (PAPD) of Jiangsu Higher Education Institutions. S.P. and Y.N. thank DARPA Grant No. HR0011727183- D18AP00010 (under the TEE Program). The authors also acknowledge the High Performance Computing Center

at the University of Arkansas and thank Jorge Íñiguez for useful discussions.

-
- [1] Baryakhtar, V. & Chupis, I. Quantum Theory of Oscillations In A Ferroelectric Ferromagnet. *Soviet Physics Solid State, USSR.* **11**, 2628+ (1970)
- [2] Smolenskii, G. & Chupis, I. Ferroelectromagnets. *Soviet Physics Uspekhi.* **25**, 475-493 (1982), <http://stacks.iop.org/0038-5670/25/i=7/a=R02?key=crossref.14140c0267d9f2ea3f559dade150f3df>
- [3] Pimenov, A., Rudolf, T., Mayr, F., Loidl, A., Mukhin, A. & Balbashov, A. Coupling of phonons and electromagnons in GdMnO₃. *Physical Review B.* **74**, 100403 (2006), <https://link.aps.org/doi/10.1103/PhysRevB.74.100403>
- [4] Pimenov, A., Mukhin, A., Ivanov, V., Travkin, V., Balbashov, A. & Loidl, A. Possible evidence for electromagnons in multiferroic manganites. *Nature Physics.* **2**, 97-100 (2006), <http://www.nature.com/articles/nphys212>
- [5] Rovillain, P., Cazayous, M., Gallais, Y., Measson, M., Sacuto, A., Sakata, H. & Mochizuki, M. Magnetic Field Induced Dehybridization of the Electromagnons in Multiferroic TbMnO₃. *Physical Review Letters.* **107**, 027202 (2011), <https://link.aps.org/doi/10.1103/PhysRevLett.107.027202>
- [6] Sushkov, A., Aguilar, R., Park, S., Cheong, S. & Drew, H. Electromagnons in Multiferroic YMn₂O₅ and TbMn₂O₅. *Physical Review Letters.* **98**, 027202 (2007), <https://link.aps.org/doi/10.1103/PhysRevLett.98.027202>
- [7] Sushkov, A., Mostovoy, M., Valdés Aguilar, R., Cheong, S. & Drew, H. Electromagnons in multiferroic RMn₂O₅ compounds and their microscopic origin. *Journal Of Physics: Condensed Matter.* **20**, 434210 (2008), <https://iopscience.iop.org/article/10.1088/0953-8984/20/43/434210>
- [8] Stanislavchuk, T., Wang, Y., Janssen, Y., Carr, G., Cheong, S. & Sirenko, A. Magnon and electromagnon excitations in multiferroic DyFeO₃. *Physical Review B.* **93**, 094403 (2016), <http://link.aps.org/doi/10.1103/PhysRevB.93.054113>
- [9] Cazayous, M., Gallais, Y., Sacuto, A., Sousa, R., Lebeugle, D. & Colson, D. Possible Observation of Cycloidal Electromagnons in BiFeO₃. *Physical Review Letters.* **101**, 037601 (2008), <https://link.aps.org/doi/10.1103/PhysRevLett.101.037601>

- [10] Rovillain, P., Cazayous, M., Gallais, Y., Sacuto, A., Lobo, R., Lebeugle, D. & Colson, D. Polar phonons and spin excitations coupling in multiferroic BiFeO₃ crystals. *Physical Review B*. **79**, 180411 (2009), <https://link.aps.org/doi/10.1103/PhysRevB.79.180411>
- [11] Skiadopoulou, S., Goian, V., Kadlec, C., Kadlec, F., Bai, X., Infante, I., Dkhil, B., Adamo, C., Schlom, D. & Kamba, S. Spin and lattice excitations of a BiFeO₃ thin film and ceramics. *Physical Review B*. **91**, 174108 (2015), <https://link.aps.org/doi/10.1103/PhysRevB.91.174108>
- [12] Lebeugle, D., Colson, D., Forget, A., Viret, M., Bonville, P., Marucco, J. & Fusil, S. Room-temperature coexistence of large electric polarization and magnetic order in BiFeO₃ single crystals. *Physical Review B*. **76**, 024116 (2007), <http://link.aps.org/doi/10.1103/PhysRevB.76.024116>
- [13] Sousa, R. & Moore, J. Electrical control of magnon propagation in multiferroic BiFeO₃ films. *Applied Physics Letters*. **92**, 022514 (2008), <http://aip.scitation.org/doi/10.1063/1.2835704>
- [14] Chang, C., Mani, B., Lisenkov, S. & Ponomareva, I. Prediction of electromagnons in antiferromagnetic ferroelectrics from first-principles: The case of BiFeO₃. *Ferroelectrics*. **494**, 68-75 (2016), <http://www.tandfonline.com/doi/abs/10.1080/00150193.2016.1137470>
- [15] Seki, S., Kida, N., Kumakura, S., Shimano, R. & Tokura, Y. Electromagnons in the Spin Collinear State of a Triangular Lattice Antiferromagnet. *Physical Review Letters*. **105**, 097207 (2010), <https://link.aps.org/doi/10.1103/PhysRevLett.105.097207>
- [16] Chen, H., Li, Y. & Berakdar, J. Electric-field control of electromagnon propagation and spin-wave injection in a spiral multiferroic/ferromagnet composite. *Journal Of Applied Physics*. **117** (2015), <http://dx.doi.org/10.1063/1.4906520>
- [17] Davydova, M., Zvezdin, K., Mukhin, A. & Zvezdin, A. Spin dynamics, antiferrodistortion and magnetoelectric interaction in multiferroics. The case of BiFeO₃. *Physical Sciences Reviews*. **5**, 1-15 (2020), <https://www.degruyter.com/document/doi/10.1515/psr-2019-0070/html>
- [18] Sayedaghaee, S., Prosandeev, S., Prokhorenko, S., Nahas, Y., Paillard, C., Xu, B. & Bellaiche, L. Domain-wall-induced electromagnons in multiferroics. *Physical Review Materials*. **6**, 034403 (2022), <https://link.aps.org/doi/10.1103/PhysRevMaterials.6.034403>
- [19] Sayedaghaee, S., Xu, B., Prosandeev, S., Paillard, C. & Bellaiche, L. Novel dynamical magnetoelectric effects in multiferroic BiFeO₃. *Physical Review Letters*. **122**, 097601 (2019)
- [20] Sayedaghaee, S., Paillard, C., Prosandeev, S., Xu, B. & Bellaiche, L. Strain-induced resonances in the dynamical quadratic magnetoelectric response of multiferroics. *Npj Computational Ma-*

- terials*. **6**, 1-6 (2020)
- [21] Stenberg, M. & Sousa, R. Model for twin electromagnons and magnetically induced oscillatory polarization in multiferroic $RMnO_3$. *Physical Review B*. **80**, 094419 (2009), <https://link.aps.org/doi/10.1103/PhysRevB.80.094419>
- [22] Lachheb, M., Zhu, Q., Fusil, S., Wu, Q., Carrétéro, C., Vecchiola, A., Bibes, M., Martinotti, D., Mathieu, C., Lubin, C., Pancotti, A., Li-Bourrelier, X., Gloter, A., Dkhil, B., Garcia, V. & Barrett, N. Surface and bulk ferroelectric phase transition in super-tetragonal $BiFeO_3$ thin films. *Physical Review Materials*. **5**, 024410 (2021), <https://doi.org/10.1103/PhysRevMaterials.5.024410>
- [23] Cherifi, S., Hertel, R., Fusil, S., Béa, H., Bouzehouane, K., Allibe, J., Bibes, M. & Barthélémy, A. Imaging ferroelectric domains in multiferroics using a low-energy electron microscope in the mirror operation mode. *Physica Status Solidi (RRL) - Rapid Research Letters*. **4**, 22-24 (2010,2), <https://onlinelibrary.wiley.com/doi/10.1002/pssr.200903297>
- [24] Gruverman, A., Alexe, M. & Meier, D. Piezoresponse force microscopy and nanoferroic phenomena. *Nature Communications*. **10**, 1661 (2019), <http://dx.doi.org/10.1038/s41467-019-09650-8>
- [25] Kholkin, A., Kalinin, S., Roelofs, A. & Gruverman, A. Review of Ferroelectric Domain Imaging by Piezoresponse Force Microscopy. *Scanning Probe Microscopy*. **2** pp. 173-214 (2007)
- [26] Prosandeev, S., Wang, D., Ren, W., Íñiguez, J. & Bellaiche, L. Novel nanoscale twinned phases in perovskite oxides. *Advanced Functional Materials*. **23**, 234-240 (2013)
- [27] Prosandeev, S., Yang, Y., Paillard, C. & Bellaiche, L. Displacement current in domain walls of bismuth ferrite. *Npj Computational Materials*. **4**, 1-9 (2018)
- [28] Wang, D., Weerasinghe, J. & Bellaiche, L. Atomistic molecular dynamic simulations of multiferroics. *Physical Review Letters*. **109**, 067203 (2012)
- [29] García-Palacios, J. & Lázaro, F. Langevin-dynamics study of the dynamical properties of small magnetic particles. *Physical Review B*. **58**, 14937 (1998)
- [30] Hlinka, J., Paściak, M., Körbel, S. & Marton, P. Terahertz-range polar modes in domain-engineered $BiFeO_3$. *Physical Review Letters*. **119**, 057604 (2017)
- [31] Xu, B., Íñiguez, J. & Bellaiche, L. Designing lead-free antiferroelectrics for energy storage. *Nature Communications*. **8**, 1-8 (2017)

- [32] Boyn, S., Grollier, J., Lecerf, G., Xu, B., Locatelli, N., Fusil, S., Girod, S., Carrétéro, C., Garcia, K., Xavier, S., Tomas, J., Bellaiche, L., Bibes, M., Barthélémy, A., Saïghi, S. & Garcia, V. Learning through ferroelectric domain dynamics in solid-state synapses. *Nature Communications*. **8**, 14736 (2017), <http://www.nature.com/articles/ncomms14736>
- [33] Rovillain, P., De Sousa, R., Gallais, Y., Sacuto, A., Méasson, M., Colson, D., Forget, A., Bibes, M., Barthélémy, A. & Cazayous, M. Electric-field control of spin waves at room temperature in multiferroic BiFeO₃. *Nature Materials*. **9**, 975-979 (2010)
- [34] Cazayous, M., Malka, D., Lebeugle, D. & Colson, D. Electric field effect on Bi Fe O₃ single crystal investigated by Raman spectroscopy. *Applied Physics Letters*. **91**, 071910 (2007)
- [35] Lobo, R., Moreira, R., Lebeugle, D. & Colson, D. Infrared phonon dynamics of a multiferroic BiFeO₃ single crystal. *Physical Review B*. **76**, 172105 (2007)
- [36] Haumont, R., Kreisel, J., Bouvier, P. & Hippert, F. Phonon anomalies and the ferroelectric phase transition in multiferroic BiFeO₃. *Physical Review B*. **73**, 132101 (2006)
- [37] Kamba, S., Nuzhnyy, D., Savinov, M., Šebek, J., Petzelt, J., Prokleška, J., Haumont, R. & Kreisel, J. Infrared and terahertz studies of polar phonons and magnetodielectric effect in multiferroic BiFeO₃ ceramics. *Physical Review B*. **75**, 024403 (2007)

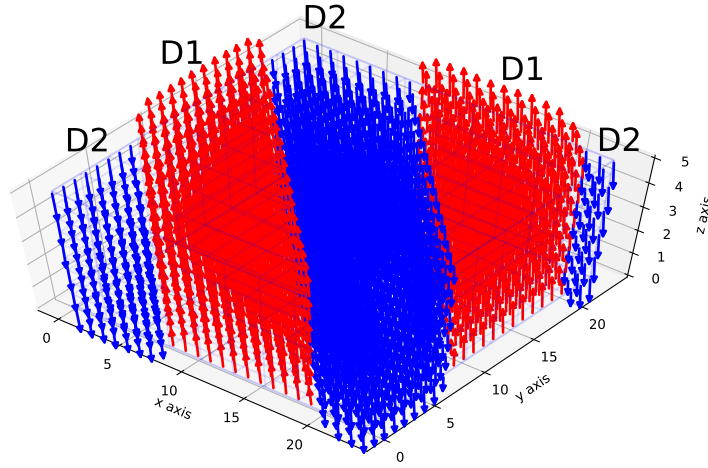


FIG. 1: (Color online) Schematic representation of the zero-field electric dipole moments' pattern for our studied $24 \times 24 \times 6$ supercell of BiFeO_3 . The blue and red vectors are used to represent electric dipole moments along the $[1\bar{1}\bar{1}]$ and $[\bar{1}11]$ directions, respectively.

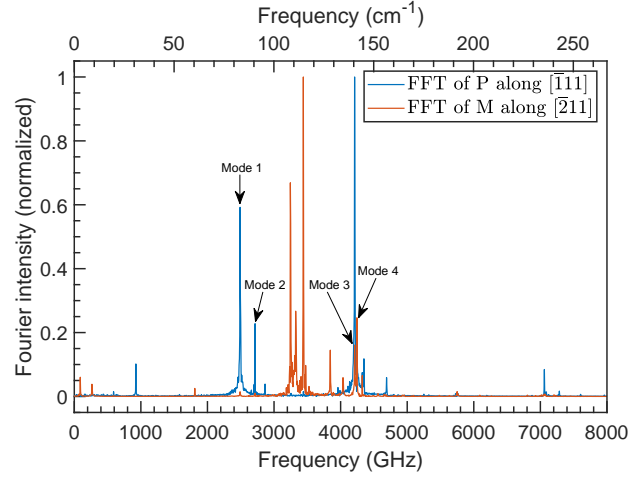


FIG. 2: (Color online) Fourier analyses of polarization and magnetization. The frequency spectrum of the component of electrical dipole moments along the $[\bar{1}11]$ direction (blue) and magnetic moments along the $[211]$ direction (orange) obtained by Fourier analysis when the applied dc electric field is $1 \times 10^7 V/m$. The frequency of the modes shown by black arrows significantly shifts upon applying different magnitudes of electric field.

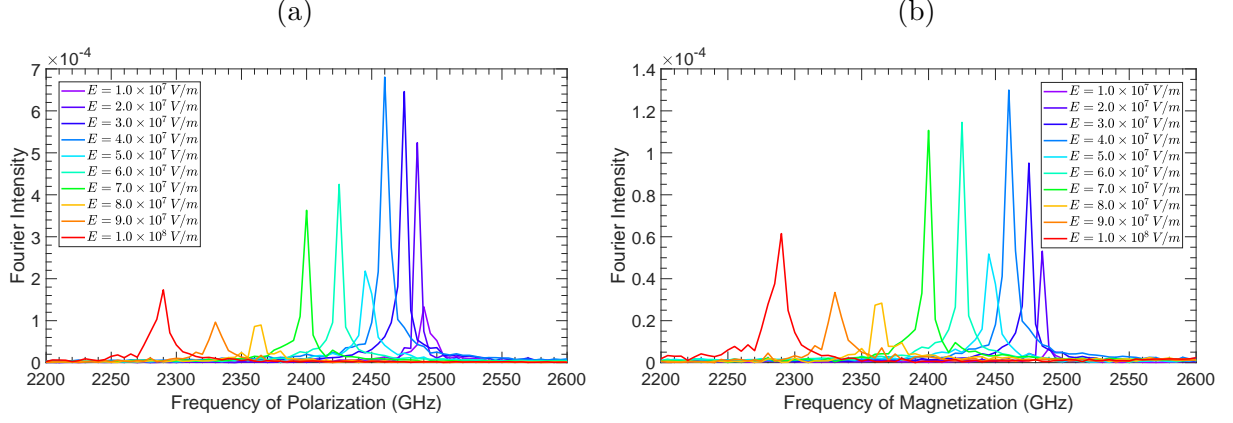


FIG. 3: (Color online) Frequency shift of optical phonons and magnons of Mode 1. (a) The shift of the frequency observed for the optical phonons upon the application of various *dc* electric fields. (b) The shift of the frequency observed for the magnons upon the application of various *dc* electric fields. For both cases the applied electric field changes from 1.0×10^7 V/m to 1.0×10^8 V/m.

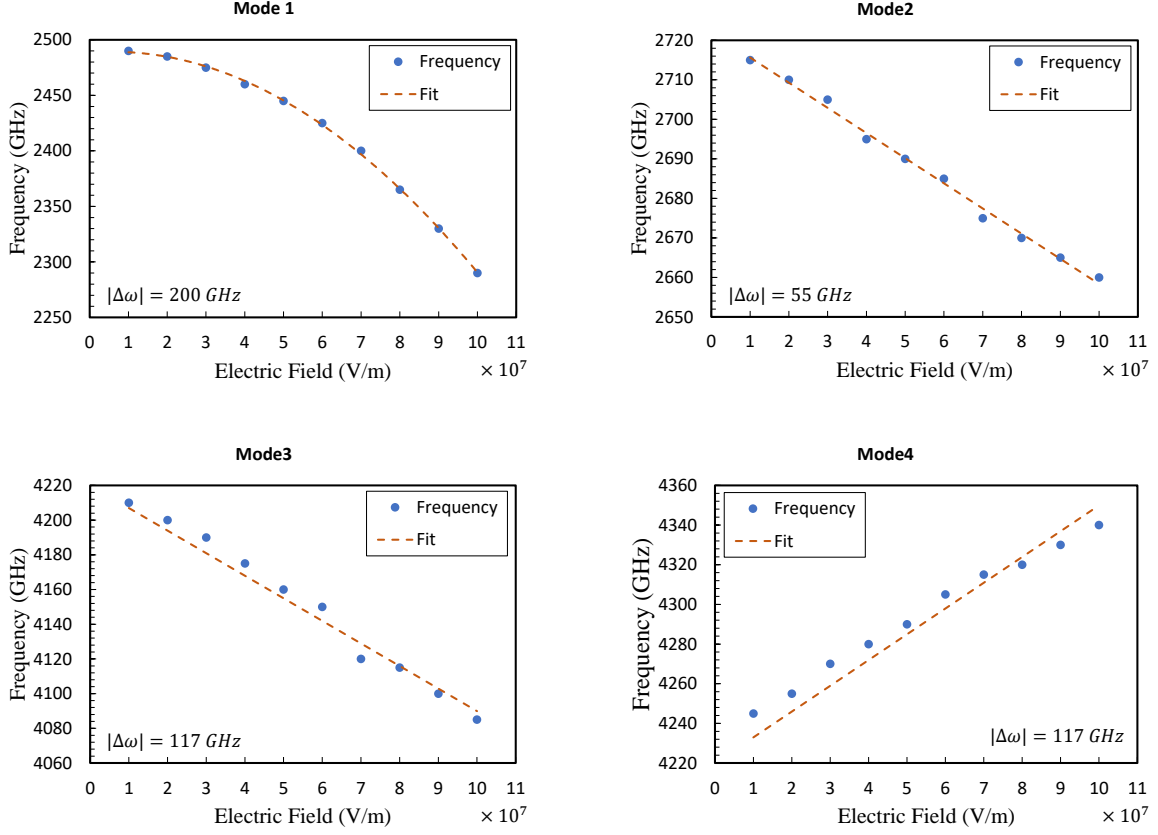


FIG. 4: (Color online) Frequency shift of four electromagnons. In each panel, the frequency shift of the corresponding mode *versus* the applied electric fields is shown. A polynomial fit of second order for Mode 1, and of first order for Modes 2, 3, and 4 is applied. $|\Delta\omega|$ is the magnitude of the difference between the highest and the lowest frequencies of the fitted lines for our chosen range of applied electric fields.

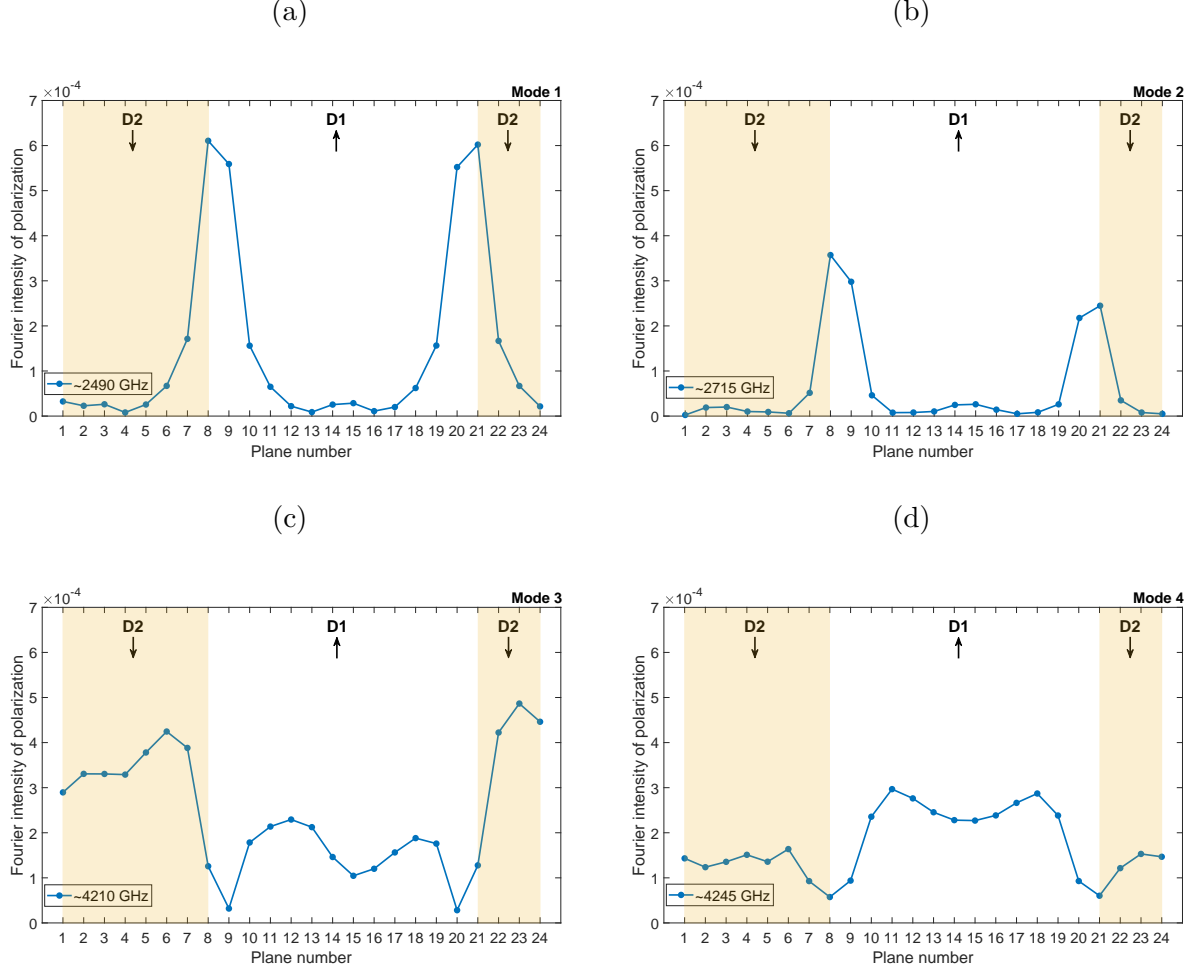


FIG. 5: (Color online) The degree of localization of the electromagnons possessing significant frequency shift under the application of electric fields. In each panel, the degree of localization of the corresponding mode at the planes parallel to the domain walls within the investigated supercell is shown. The shaded area corresponds to the domains possessing electric dipoles pointing along the $[1\bar{1}\bar{1}]$ direction, while the white area corresponds to the domains possessing electric dipoles pointing along the opposite $[\bar{1}11]$ direction. The arrow in each domain indicates the direction of the z-component of electric dipole moments present in the domain. The applied electric field for all cases is $E = 1.0 \times 10^7 \text{ V/m}$ along the $[\bar{1}11]$ direction which is parallel to the direction of the electric dipoles in D1 and antiparallel to the direction of the electric dipoles in D2.